DOI:10.20113/j.ccpr.2020.03.013

Changes of the Thermal Environment Caused by a City-Wide Lockdown: The Case of Wuhan City

Cai Zhi, Tang Yan, Zhan Qingming
Edited by Li Caige / Proofread by Mao Qizhi

Abstract The impact of the COVID-19 epidemic in Wuhan caused the city to go into a lockdown in January, 2020, and most outdoor activities stopped, which provided a chance to investigate the impact of human activities on the urban thermal environment. Using the land surface temperature (LST) and population distribution data, this paper analyzes the changes between normal workdays and the lockdown period. The results show that maximum population and LST changes can be seen in industrial and commercial areas, and the LST hot spots shrink and cold spots expand in many areas during the lockdown, which identifies that the impact of the lockdown on the urban thermal environment varies according to different types of lands. However, it should be noted that the LST has a similar spatial distribution during the two periods, in spite of the significant changes in population size. Compared with population size, the urban morphology indicators have a higher correlation with the LST. This indicates that the urban thermal environment is dominated by urban morphology, and the influence of human activities on it is still limited. All findings can help urban planners to improve the existing methods to address both climate change and public health issues.

Keywords urban thermal environment; land surface temperature (LST); population; human activities; Wuhan

1. Introduction

With the rapid development of urbanization around the world, 54% of the population is now living in urban areas, and this number will rise to 70% by 2050 (UN, 2014). As large population surges to urban areas, urban space continues to expand, and the original natural surface cover (e.g., green spaces and wetlands) has been transformed into impervious construction surfaces (e.g., buildings, paved areas, and roads). As a result, urban areas have more anthropogenic heat release than the previous, and more solar radiation is absorbed with the increase of impervious land surfaces. Thus, urban areas have higher temperatures than their surrounding rural areas (Son, Chen, Chen, Thanh, and Vuong, 2017; Kotharkar, Ramesh, and Bagade, 2018), which is known as the urban heat island (UHI) effect. The UHI effect has become significant in recent years and will be even worse in the next few decades (Lindsey, 2014; Sippel, Meinshausen, Fischer, et al., 2020). Many studies have identified that the UHI significantly influences urban sustainable development, such as causing greater energy consumption (Shen, Chow, and Darkwa, 2013; Wilson, 2013) and deteriorating air quality (Kalisa, Fadlallah, Amani, et al., 2018). Moreover, the increase in temperature can endanger vulnerable people, such as the elderly people, children, and patients (Rydin et al., 2012; Zhang, Zheng, and Chen, 2019; Mora et al., 2017; Yang et al., 2019; Cai, Tang, Chen, et al., 2019). Therefore, there is a growing need to study the UHI effect so that cities can mitigate it.

Previous studies have found that solar radiation and anthropogenic heat release are the two main sources of urban heat (Erell and Williamson, 2012). The land surface absorbs solar radiation, and the physical characteristics of land cover determine how much solar energy will be converted and released as heat. These physical characteristics of the land surface include the urban spatial structure, the type of surface material and land coverage (Sun and Chen, 2012; Cai, Han, and Chen, 2018; Xu et al., 2017; Wong et al., 2011; Guo et al., 2016; Tong et al., 2018). Regarding the urban spatial structure, several factors are widely used, such as building density (BD), building height, and sky view. Studies have also identified that a high building density and sky view can lead to a high surface temperature (Guo et al., 2016; Liu, Zhan, Gao, and Yang, 2019) and a negative relationship between the building height and surface temperature (Yang and Li, 2015). Land cover material refers to the roof materials and surface colors. Green roofs can decrease the building energy use and reduce the LST, while metal roof elements and dark colors above the surface can absorb more solar energy (Susca, 2019; Gao, Shi, Levinson, et al., 2017; Hsieh, Aramaki, and Hanaki, 2007). Land cover refers to pervious surfaces (e.g., green spaces and water bodies) and impervious surfaces (e.g., paved areas and roads). Pervious surfaces can cool the city due to their high heat capacity (Ferreira and Duarte, 2019; Gunawardena, Wells, and Kershaw, 2017), and impervious surfaces can warm the city due to their low reflectivity and heat capacity (Yuan and Bauer, 2007). Based on the above findings, several methods were proposed to mitigate UHI effects and enhance urban resilience, such as optimizing the urban spatial structure (Middel, Häb, Brazel, et al., 2014) and adding more green spaces and water bodies (Du, Song, Jiang, et al., 2016; Qiu and Jia, 2020; Cai et al., 2018).

Anthropogenic heat release is another urban heat source. They are influenced by population density (Manoli et al., 2019), energy

中国知网 https://www.cnki.net

consumption (Rossi, Bonamente, Nicolini, et al., 2016), and socio-economic conditions. However, it should be noted that those factors are complex, not only because they have various spatiotemporal distributions in different cities, but also because they do not directly impact urban physical factors (e.g., urban spatial form and land cover). Thus, it is difficult to study the relationship between human activities and the urban thermal environment, as well as to isolate anthropogenic heat from physical factors. For this reason, most previous studies have not considered anthropogenic heat release, and just combined it with solar radiation. Fortunately, some urban climate models (e.g., ENVI-met, WRF) have provided a window to study the impact of anthropogenic heat release on the urban thermal environment (Cao, Wu, Liu, et al., 2019; Mirzaei, 2015). However, it should be noted that those models simulate the built area in a virtual environment with ideal conditions. Few studies have assessed these effects in the real built environment, especially on the urban mesoscale.

The COVID-19 in Wuhan has suspended numerous human activities, and changed the spatial distribution of population due to the lockdown. Most residents kept staying at home, and few people went to commercial centers and factories, which provided a unique environment for comparing and assessing the influence of human activities on the urban thermal environment. Thus, in this study, two Landsat images, one from a typical workday and one taken during the lockdown period, are used to compare the spatial temperature differences, so as to explore the following issues: ① What thermal environmental differences are there during the city-wide lockdown? ② What is the impact of human activities on the urban thermal environment?

2. Data and methods

2.1 Study area

Wuhan City, the capital of Hubei Province, is located in eastern Hubei Province between 29°58′ – 31°22′ north latitude and 113°41′– 115°05′ east longitude (see Figure 1). According to the local historical meteorological data, its annual average air temperature ranges from 15.8 °C to 17.5 °C, and its highest air temperature can reach 40 °C in summer, which makes it one of the "stove cities" in China. Wuhan City has 13 administrative districts with a local permanent population of 9.06 million, and a floating population that had reached 5.1 million by the end of 2019 (Wuhan Bureau of Statistics, 2020). Since most people are concentrated in the urban core areas, the following five districts are selected as the study area in this paper (Jiang'an District, Jianghan District, Qiaokou District, Hanyang District, and Wuchang District). The permanent population in these districts amounts to 4.5 million, approximately half of Wuhan's population.

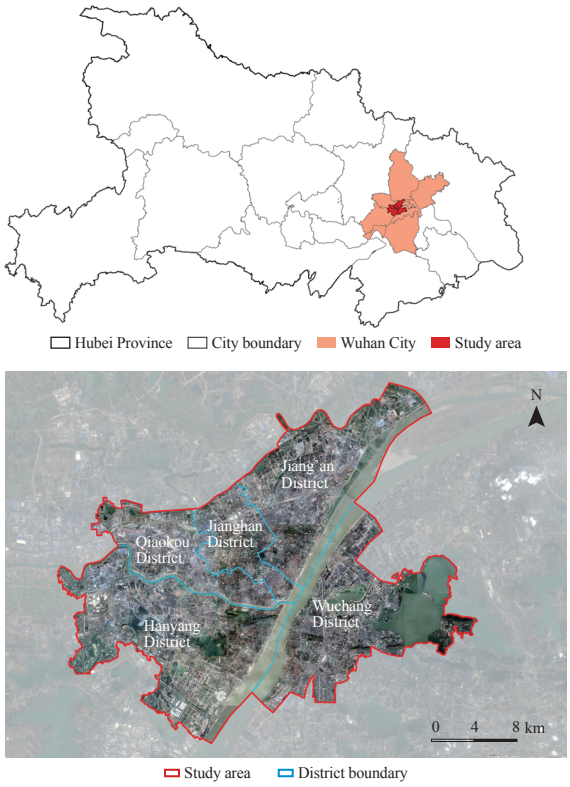


Figure 1 Location of Wuhan City and the study area

COVID-19 emerged in Wuhan City in the end of December 2019 and became an outbreak in mid-January 2020 (the State Council Information Office of the People's Republic of China, 2020). By Jun. 3, 2020, the epidemic had caused 50,340 people to be infected and resulted in 3,869 deaths in Wuhan (Wuhan Municipal Health Commission, 2020). To cut off the spread of the epidemic, Wuhan was placed in lockdown in Jan. 23, 2020, and the lockdown was lifted on Apr. 8 (the State Council Information Office of the People's Republic of China, 2020). During the lockdown period, public transportation was stopped and few residents were allowed to leave or enter the city. Outdoor activities came to a stop, and residents were required to stay at home. Moreover, before the city-wide lockdown, more than 5 million residents returned to their hometowns for the Spring Festival. Thus a significant difference could be seen in the size of the population and human activities while the city was in lockdown. The squares, parks, shops, and factories were "empty" and no longer "hot."

中国知网 https://www.cnki.net

2.2 Methodology

2.2.1 Data sources and preprocessing

Cloud-free Landsat-8 remote sensing images upon the study areas were used to retrieve land surface temperature (LST). This dataset was downloaded from the USGS website (https://earthexplorer.usgs.gov/), and images with different bands were used to calculate the normalized difference vegetation index (NDVI) and the normalized difference built-up index (NDBI). To compare the spatial differences in human activities and the changes of urban thermal environment, two remote sensing images were selected, which respectively represented a typical workday (Dec. 7, 2019) and a day during the lockdown period (Feb. 9, 2020) (see Table 1). Both days had similar weather conditions as the air temperature ranged from 0 – 15 °C. Both images were acquired at 10:56 am (local time) from path 123 and row 39.

Building information (outline, area, and floor number) was downloaded from Baidu Maps with an API tool. Compared with the Baidu population heat map, that of WeChat included more users, and its products (EasyGo) can better capture the distribution of the population. Since the EasyGo dataset did not provide historical data, we acquired the EasyGo data for Feb. 24 and Apr. 13, 2020 respectively, which represented the population distribution during the lockdown period (Feb. 24) and during a post-lockdown workday (Apr. 13) , and both were taken at 11:00 am. The land use data were downloaded from the local natural resource bureau, and Google satellite images of the study areas were retrieved from Google Earth software. All data were imported to the ArcGIS Pro (version 2.5) software for preprocessing, which included geometric correction and spatial analysis.

2.2.2 LST retrieval

The Landsat-8 TIRS band (band 10) was used to retrieve LST. In this study, we used a tool named the "Landsat-8 TIRS surface temperature inversion tool" in ENVI software (version 5.3), which is semiautomatic and can quickly obtain results, to retrieve the LST.

2.2.3 Normalized LST

To make the LST distribution comparable in different periods, the normalized LST was used. The normalized LST formula can be expressed as follows:

Table 1 LST and population data acquired time

	Normal workdays	Lockdown periods
Land surface temperature	Dec. 7, 2019	Feb. 9, 2020
Population distribution	Apr. 13, 2020	Feb. 25, 2020

$$NLST = \frac{LST - LST_{min}}{LST_{max} - LST_{min}}$$

$$ND = NLST - NLST_{min}$$

where *LST* represents the original value of the *LST* for each cell, LST_{min} is the minimum *LST* value in the study area, and LST_{max} is the maximum *LST* value in the study area. *NLST* is the normalized *LST*, and its value ranges from 0 to 1. *ND* is the normalized *LST* difference between various land uses, $NLST_{min}$ is the type of land use (forest in this study) with the minimum mean *NLST* value.

2.2.4 Hot spot analysis

Since it is difficult to directly determine the differences in the spatial distribution of LST, some high values may not be statistically significant. Thus, in this study, an optimized hot spot analysis tool in ArcGIS Pro (version 2.5) was used to explore the high/low LST clusters.

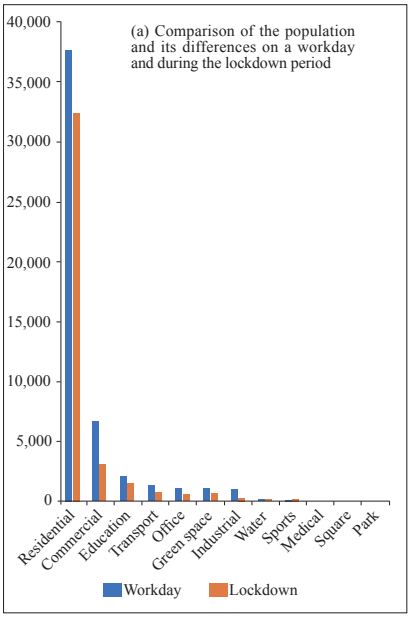
3. Results

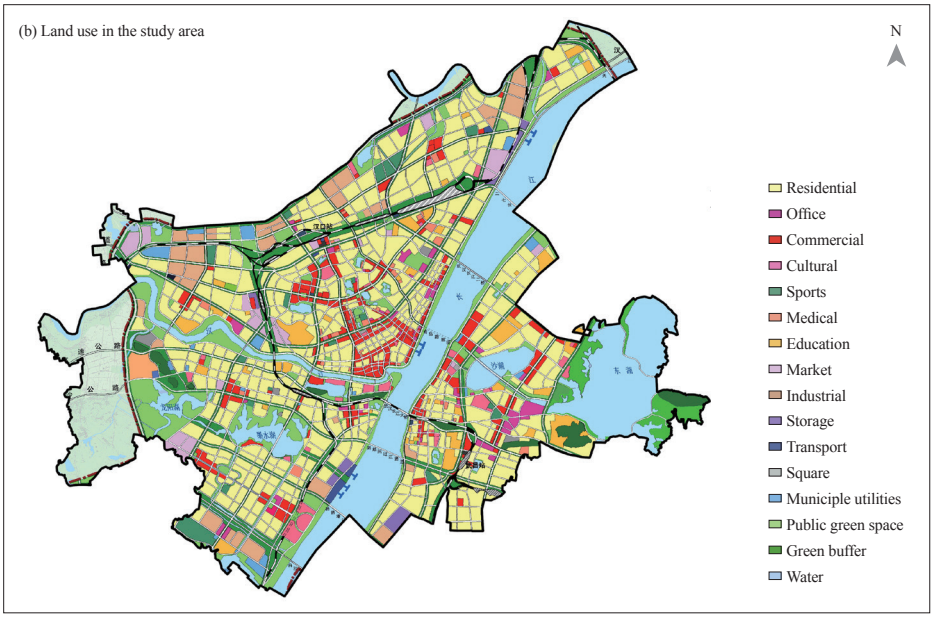
3.1 Population distribution

The population had a similar distribution in both the typical workday and the day during the lockdown period (see Figure 2). The highest population concentrations were in residential land, followed by commercial land. The high population zones were located in central Jiang'an District, southeastern Qiaokou District and Jianghan District, northern Hanyang District and southwestern Wuchang District. Most residents live along Jinghan Road, which, as the city center, has many residential communities. This land has mixed functions, like residential and commercial uses. The population distribution also showed that most outdoor activities stopped during the lockdown period, as few people came to parks and squares.

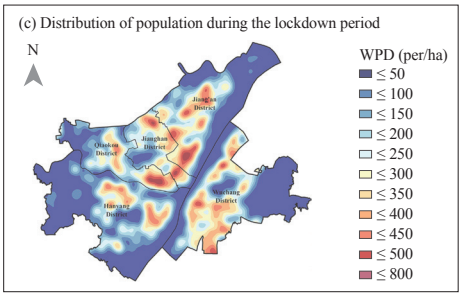
Compared with a typical workday, the population had a significantly decreasing trend during the lockdown period due to the Spring Festival and epidemic impact, except the sports land (see Figure 2a). Among the sports land, seven gymnasiums were turned to temporary treatment centers during the lockdown period and offered thousands of beds for patients. During this period, these areas had more people than on typical workdays. With regard to medical land, hospitals housed almost only COVID-19 patients, and many ordinary patients had to return home. This resulted in a significant population difference during the lockdown periods. The shops and factories were shut down during the city-wide lockdown, and the population on those lands also significantly decreased. Regarding office and transportation land, most of the facilities were shut down, although some government departments and facilities continued to

中国知网 https://www.cnki.net





Land use	Workday	Lockdown	Differences (%)
Residential	37,713	32,459	16.19
Commercial	6,683	3,108	115.03
Education	2,209	1,581	39.72
Transport	1,370	760	80.26
Office	1,203	665	80.90
Green space	1,062	671	58.27
Industrial	1,032	373	176.68
Water	174	110	58.18
Sports	139	272	-48.90
Medical	86	25	244.00
Square	56	12	366.67
Park	49	24	104.17



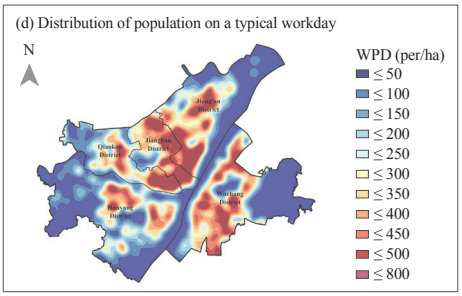


Figure 2 Land use and population distribution

run during the lockdown period. Thus, the population differences in these areas were lower than those of industrial and commercial lands. Educational and residential lands had smaller population differences. When the population data was acquired on Apr. 13, 2020, schools remained closed and all students still stayed at home during this period.

3.2 Distribution of LST

3.2.1 LST distribution

The LST showed a similar spatial distribution during the two periods (see Figures 3a & 3b), and strong Pearson correlations between the typical workday (Dec. 7) and the lockdown period (Feb. 9) were also identified (0.89**, $P < 0.01$). The high LST values were distributed in western Hanyang District, central Qiaokou District, and northeastern Jiang'an District. The land use type in those areas consists of mainly industrial land, and the building roofs are covered by dark and metal materials, which are easily heated by solar radiation. The zonal statistics results also showed that industrial and commercial lands had higher LSTs and acted as heat islands in the city (see Figure 3c); park and forest land had lower LSTs and acted as cold islands in the city.

The thermal environment showed some differences between those two periods. Even though weather conditions were similar in the two days, the lockdown period had a higher LST than the workdays (see Figure 3c). The normalized LST differences (ND) showed that the lockdown period had a smaller temperature difference than the workdays in blocks with different land uses (see Figure 3d). This meant that the thermal effect of various land uses tended to be homogenous during the city-wide lockdown. As human activities and anthropogenic heat release decreased, the impact of human activities on the urban thermal environment also decreased. The ND values in different periods also confirmed this impact, as the highest ND values decreased from commercial land (0.016) to residential

中国知网 https://www.cnki.net

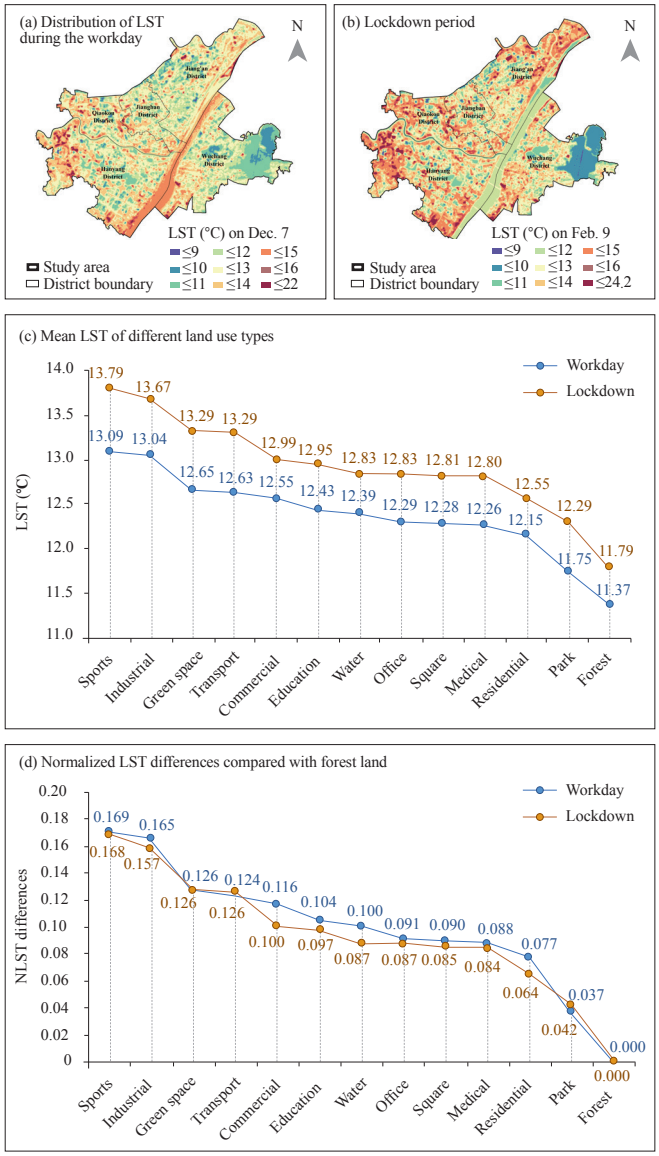


Figure 3 Distribution of LST and its differences in various land use types

land (0.013), to industrial land (0.008), and to educational land (0.007). Compared with a typical workday, those areas also had more significant population differences during the lockdown period. For the other types of land use such as office and medical lands, the ND was not significant since the distributed population was relatively small.

3.2.2 LST hot spots and cold spots

Since it was difficult to compare the LST differences directly, the Getis-Ord statistics was further used to find the hot spots and cold spots during the two periods. On the typical workday, most LST hot spots were located in western and southeastern Hanyang District, western Qiaokou District, and southwestern Wuchang District. Most LST cold spots were located in the middle of Jian'an District and Wuchang District (see Figure 4). During the lockdown period, even though the distribution of LST hot and cold spots were similar, differences still existed. The hot spots shrank in western Hanyang District and southwestern Wuchang District and disappeared in the southeast of Jianghan District, but they were expanded in northeastern Jiang'an District. Regarding the cold spots, many of the LST cold spots in Jiang'an District also disappeared and were not significant. In Hanyang District, the LST cold spots also had a different spatial distribution compared with the typical workdays. There were three cold spot clusters in the workdays, while only two cold spot clusters in the lockdown period, and those clusters were more concentrated.

During the city-wide lockdown, shops and most factories were closed, so few people went to these places. The anthropogenic heat release significantly decreased, which made the LST hot spots shrinking in some industrial parks and even disappearing in commercial centers (see Figure 4). Since residents stayed at home instead of going out, the anthropogenic heat release occurred more in homes and was concentrated in urban communities, which caused

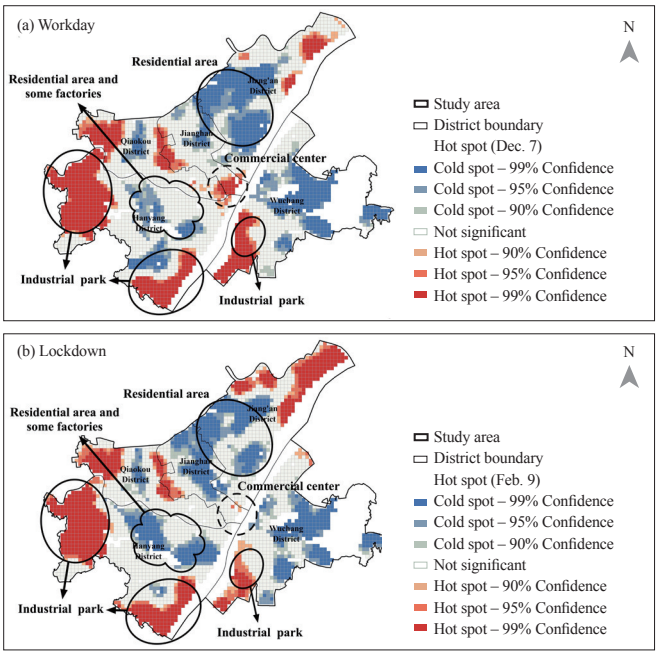


Figure 4 Distribution of LST hot spots on a workday and during the lockdown period

中国知网 https://www.cnki.net

an increase in the temperature, and the LST cold spots in the residential areas shrank compared with those on the workday. However, it should be noted that many residents had left Wuhan for the Spring Festival before the city-wide lockdown. Thus, the total number of residents and anthropogenic heat release were reduced in some communities, which may have resulted in a higher number of LST cold spots that appeared in the north of Hanyang District.

4. Discussion

4.1 Correlations between urban structural factors and LST

To further explore the thermal environment differences since the city-wide lockdown, the correlations between some urban structural factors and LST were analyzed (see Table 2). The results showed that NDBI and BD had a significant positive relationship with the LST. However, those correlations decreased during the lockdown period compared with normal workdays, as the NDBI coefficient relationship decreased from 0.575** (workday) to 0.507** (lockdown), and the BD coefficient relationship decreased from 0.040** (workday) to -0.016 (lockdown). The NDBI and BD reflected the percentages of impervious surface coverage; the higher the NDBI and BD value, the more buildings and human activities in those areas. During the lockdown period, the population size decreased significantly as numerous residents had already left Wuhan City and few outdoor activities occurred, which could have reduced anthropogenic heat release. Impervious surfaces mainly received energy from solar radiation. Thus, the correlations between NDBI, BD, and LST showed a decreasing trend.

NDVI had a significant positive relationship with LST, which increased during the city-wide lockdown (see Table 2). The NDVI reflected the coverage of natural green elements. As the population and human activities decreased in green spaces, the interference of anthropogenic heat release on the relationship between the NDVI and LST also decreased. The positive relationship can be explained by the thermal properties of water bodies, as NDVI values below 0 represented that water bodies were related to low LST. Moreover, the study area had numerous water bodies, and the thermal effects of water bodies can cover a large percentage of the urban area and modify the relationship between NDVI and LST (Cai et al., 2018).

4.2 Comparison of the impact of anthropogenic heat release and solar radiation on the urban thermal environment

Solar radiation plays a vital role in urban microclimates, and LST is influenced by land cover, especially its heat characteristics. The LST distribution showed that high LST values appeared in the industrial land, while low LST values appeared in green spaces. Although the hot spot analysis showed some spatial distribution differences between hot spots and cold spots, those differences were not significant, which was caused by the different spatial distributions of the population and human activities. Even though the weather conditions were similar in the two days of remote-sensing data that were used, the lockdown period had a higher LST than the workday. The rise of the LST during the lockdown period can be explained by the decreased NDVI value in those areas (see Figure 5). Since the data of Dec. 7, 2019 was used to represent the workdays in winter, it should be noted that most leaves did not fall and the green space remained yellow or even green in early December. Most of those green colors were dispersed in early February, as the autumn had been over for several months. Trees no longer created shadows, and solar radiation directly reached the ground and heated the land surface.

Table 2 Pearson coefficient relationship between urban structural factors and LST

Urban structural factors	Workday	Lockdown
NDBI	0.575**	0.507**
NDVI	0.280**	0.360**
BD	0.040**	-0.016

Note: ** represents significant at 0.01 level.

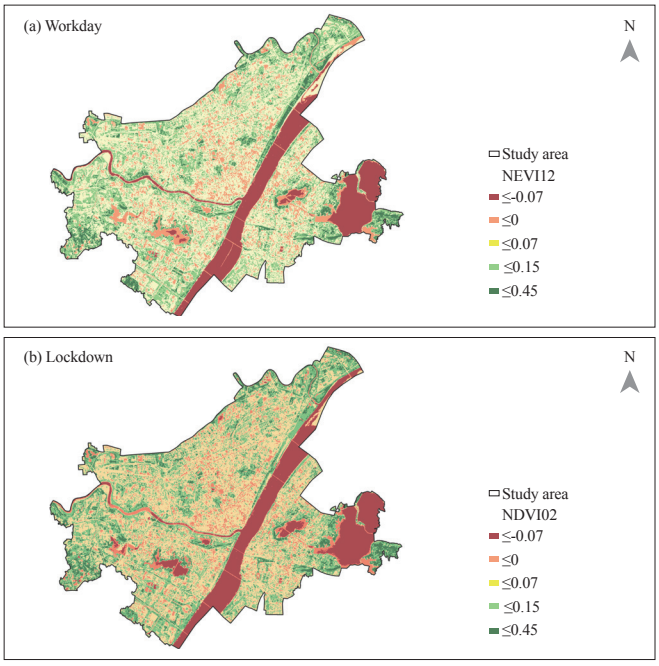


Figure 5 Distribution of NDVI during the workday and lockdown period

中国知网 https://www.cnki.net

Anthropogenic heat release has a weaker impact on LST than solar radiation, and its contribution to the urban thermal environment is complex. Anthropogenic heat release is caused by human activities, which has numerous factors, such as energy use, population, climate, and even human behavior. In terms of energy use, industrial activities and transportation activities consume more energy and release more heat than residential activities. In terms of population, the population size and its characteristics (e.g., income, gender, age) can also influence energy consumption, which can affect the distribution of anthropogenic heat release and the urban thermal environment. In terms of climate, more anthropogenic heat is released in summer and winter due to cooling and warming needs. Other than these factors, it is still difficult to directly determine the impact of anthropogenic heat release on land surface, as the heat released by human activities is transmitted by air. Since there are many tall residential buildings in Wuhan, residential activities slightly impacted the LST.

However, these findings did not illustrate that the influence of human activities on the urban thermal environment can be ignored. In contrast, more attention should be paid on the activities that occurred in buildings, as most energy was consumed in buildings. In addition, reducing the energy consumption in buildings may also be an effective way to mitigate UHIs, reduce the impacts of human activities on the urban thermal environment, and allow the city to cope with climate change.

5. Conclusion

In this study, we compared the population and urban thermal environmental differences in Wuhan City between a typical workday and the lockdown period in winter. The results showed that the population had a similar spatial distribution during the city-wide lockdown. As numerous residents went back to their hometowns for the Spring Festival, the population decreased in most areas. Combined with the effect of the epidemic, the population in industrial and commercial areas significantly decreased. Compared with that on a normal workday, a significant temperature difference also appeared in the industrial and commercial areas. However, the LST had a similar spatial distribution during the city-wide lockdown period.

The above findings illustrated that the anthropogenic heat released by human activities had a weaker impact on the urban thermal environment than solar radiation. Thus, optimizing the urban spatial form and reducing the absorption capacity of land surface to solar radiation can be regarded as effective ways to improve the urban thermal environment. Since the urban thermal environment was also influenced by human activities, especially in the urban land use with high population density and energy consumption, planners and policymakers should also pay attention to those areas, and mitigate the impact of human activities on the urban thermal environment by reducing energy consumption and anthropogenic heat release, so as to increase the urban thermal resilience and make it better adapt to the climate change. C

References:

Cai Z, Han G, and Chen M (2018). Do Water Bodies Play an Important Role in the Relationship Between Urban Form and Land Surface Temperature? *Sustainable Cities and Society*, 39, pp. 487 – 498.

Cai Z, Tang Y, Chen K, and Han G (2019). Assessing the Heat Vulnerability of Different Local Climate Zones in the Old Areas of a Chinese Megacity. *Sustainability*, 11 (7), p. 2032.

Cao Z, Wu Z, Liu L, Chen Y, and Zou Y (2019). Assessing the Relationship Between Anthropogenic Heat Release Warming and Building Characteristics in Guangzhou: A Sustainable Development Perspective. *Science of the Total Environment*, 695, 133759. Available at: <https://doi.org/10.1016/j.scitotenv.2019.133759>.

Du H, Song X, Jiang H, Kan Z, Wang Z, and Cai Y (2016). Research on the Cooling Island Effects of Water Body: A Case Study of Shanghai, China. *Ecological Indicators*, 67, pp. 31 – 38.

Erell E, Pearlmutter D, and Williamson T (2012). *Urban Microclimate: Designing the Spaces Between Buildings*. New York: Routledge.

Ferreira L S and Duarte D H S (2019). Exploring the Relationship Between Urban Form, Land Surface Temperature and Vegetation Indices in a Subtropical Megacity. *Urban Climate*, 27, pp. 105 – 123.

Gao Y, Shi D, Levinson R, Guo R, Lin C, and Ge J (2017). Thermal Performance and Energy Savings of White and Sedum-Tray Garden Roof: A Case Study in a Chongqing Office Building. *Energy and Buildings*, 156, pp. 343 – 359.

Gunawardena K R, Wells M J, and Kershaw T (2017). Utilising Green and Bluespace to Mitigate Urban Heat Island Intensity. *Science of the Total Environment*, 584, pp. 1040 – 1055.

Guo G, Zhou X, Wu Z, Xiao R, and Chen Y (2016). Characterizing the Impact of Urban Morphology Heterogeneity on Land Surface Temperature in Guangzhou, China. *Environmental Modelling & Software*, 84, pp. 427 – 439.

Hsieh C M, Aramaki T, and Hanaki K (2007). Estimation of Heat Rejection Based on the Air Conditioner Use Time and Its Mitigation from Buildings in Taipei City. *Building and Environment*, 42 (9), pp. 3125 – 3137.

Kalisa E, Fadlallah S, Amani M, Nahayo L, and Habiyaremye G (2018). Temperature and air Pollution Relationship During Heatwaves in Birmingham, UK. *Sustainable Cities and Society*, 43, pp. 111 – 120.

Kotharkar R, Ramesh A, and Bagade A (2018). Urban Heat Island Studies in South Asia: A Critical Review. *Urban Climate*, 24, pp. 1011 – 1026.

Lindsey R (2014). How Much will Earth Warm If Carbon Dioxide Doubles Pre-Industrial Levels? Availabe at: <www.climate.gov>. Jan. 24.

Liu H, Zhan Q, Gao S, and Yang C (2019). Seasonal Variation of the Spatially Non-Stationary Association Between Land Surface Temperature and Urban

中国知网 https://www.cnki.net

Landscape. *Remote Sensing*, 11 (9), p. 1016.

Manoli G, Fatichi S, Schläpfer M, Yu K, Crowther T W, Meili N, et al. (2019). Magnitude of Urban Heat Islands Largely Explained by Climate and Population. *Nature*, 573, pp. 55 – 60.

Middel A, Häb K, Brazel A J, Martin C A, and Guhathakurta S (2014). Impact of Urban Form and Design on Mid-Afternoon Microclimate in Phoenix Local Climate Zones. *Landscape and Urban Planning*, 122, pp. 16 – 28.

Mirzaei P A (2015). Recent Challenges in Modeling of Urban Heat Island. *Sustainable Cities and Society*, 19, pp. 200 – 206.

Mora C, Dousset B, Caldwell I R, Powell F E, Geronimo R C, Bielecki C R, et al. (2017). Global Risk of Deadly Heat. *Nature Climate Change*, 7 (7), pp. 501 – 506.

Qiu K and Jia B (2020). The Roles of Landscape Both Inside the Park and the Surroundings in Park Cooling Effect. *Sustainable Cities and Society*, 52, 101864. Availabe at: <https://doi.org/10.1016/j.scs.2019.101864>.

Rossi F, Bonamente E, Nicolini A, Anderini E, and Cotana F (2016). A Carbon Footprint and Energy Consumption Assessment Methodology for UHI-Affected Lighting Systems in Built Areas. *Energy and Buildings*, 114, pp. 96 – 103.

Rydin Y, Bleahu A, Davies M, Dávila J D, Friel S, De Grandis G, et al. (2012). Shaping Cities for Health: Complexity and the Planning of Urban Environments in the 21st Century. *The Lancet*, 379 (9831), pp. 2079 – 2108.

Shen T, Chow D H C, and Darkwa J (2013). Simulating the Influence of Micro-Climatic Design on Mitigating the Urban Heat Island Effect in the Hangzhou Metropolitan Area of China. *International Journal of Low-Carbon Technologies*, available at: <http://dx.doi.org/10.1093/ijlct/ctt050>.

Sippel S, Meinshausen N, Fischer E M, Székely E, and Knutti R (2020). Climate Change Now Detectable from Any Single Day of Weather at Global Scale. *Nature Climate Change*, 10 (1), pp. 35 – 41.

Son N T, Chen C F, Chen C R, Thanh B X, and Vuong T H (2017). Assessment of Urbanization and Urban Heat Islands in Ho Chi Minh City, Vietnam Using Landsat Data. *Sustainable Cities and Society*, 30, pp. 150 – 161.

Sun R and Chen L (2012). How Can Urban Water Bodies Be Designed for Climate Adaptation?. *Landscape and Urban Planning*, 105 (1 & 2), pp. 27 – 33.

Susca T (2019). Green Roofs to Reduce Building Energy Use? A Review on Key Structural Factors of Green Roofs and Their Effects on Urban Climate. *Building and Environment*, 162, 106273. Available at: < https://doi.org/10.1016/j.buildenv.2019.106273 >.

The State Council Information Office of the People's Republic of China (2020). Fighting COVID-19: China in Action. Available at: <http://www.scio.gov.cn/zfbps/ndhf/42312/Document/1682142/1682142.htm>.

Tong S, Wong N H, Jusuf S K, Tan C L, Wong H F, Ignatius M, and Tan E (2018). Study on Correlation Between Air Temperature and Urban Morphology Parameters in Built Environment in Northern China. *Building and Environment*, 127, pp. 239 – 249.

UN (2014). *World Urbanization Prospects* (The 2014 Revision). New York: UN, Department of Economic and Social Affairs United Nations, Population Division.

Wilson B (2013). Urban Form and Residential Electricity Consumption: Evidence from Illinois, USA. *Landscape and Urban Planning*, 115, pp. 62 – 71.

Wong M S, Nichol J, and Ng E (2011). A Study of the "Wall Effect" Caused by Proliferation of High-Rise Buildings Using GIS Techniques. *Landscape and Urban Planning*, 102 (4), 245 – 253.

Wuhan Bureau of Statistics (2020). Statistical Bulletin of National Economic and Social Development of Wuhan in 2019. Available at: <http://tjj.wuhan.gov.cn/tjfw/tjgb/202004/t20200429_1191417.shtml>.

Wuhan Municipal Health Commission (2020). The Epidemic Situation of Novel Coronavirus Pneumonia in Wuhan. Available at: <http://wjw.wuhan.gov.cn/xwzx_28/gsgg/202006/t20200604_1362570.shtml>.

Xu Y, Ren C, Ma P, Ho J, Wang W, Lau K K L, et al. (2017). Urban Morphology Detection and Computation for Urban Climate Research. *Landscape and Urban Planning*, 167, pp. 212 – 224.

Yang J, Yin P, Sun J, Wang B, Zhou M, Li M, et al. (2019). Heatwave and Mortality in 31 Major Chinese Cities: Definition, Vulnerability and Implications. *Science of the Total Environment*, 649, pp. 695 – 702.

Yang X and Li Y (2015). The Impact of Building Density and Building Height Heterogeneity on Average Urban Albedo and Street Surface Temperature. *Building and Environment*, 90, pp. 146 – 156.

Yuan F and Bauer M E (2007). Comparison of Impervious Surface Area and Normalized Difference Vegetation Index as Indicators of Surface Urban Heat Island Effects in Landsat Imagery. *Remote Sensing of Environment*, 106 (3), pp. 375 – 386.

Zhang W, Zheng C, and Chen F (2019). Mapping Heat-Related Health Risks of Elderly Citizens in Mountainous Area: A Case Study of Chongqing, China. *Science of the Total Environment*, 663, pp. 852 – 866.

Authors

Cai Zhi, PhD Candidate, School of Architecture, Tsinghua University, Beijing, P. R. China.

Tang Yan (corresponding author), Associate Professor, School of Architecture, Tsinghua University, Beijing, P. R. China. Email: yantang@mail.tsinghua.edu.cn

Zhan Qingming, Professor, School of Urban Design, Wuhan University, Wuhan, P. R. China.

中国知网 https://www.cnki.net